74-GT-121

an ASME publication

On the Energy Transfer in Centrifugal Compressors

K. BAMMERT

Director

M. RAUTENBERG

Chief of Department for Radial Compressors
Institut of Turbomachinery and Gasdynamics,
University of Hanover,
Hanover, West Germany

In the layout and calculation of centrifugal compressors there are still considerable uncertainties when it comes to the theoretical determination of energy transfer from the impeller to the flowing medium and to the subsequent energy conversion in the diffuser. These problems arise particularly where compressor stage design with high pressure ratios and mass flow rates are concerned. A solution to these questions can presumably be found only through a physically balanced interpretation of the extremely complex flow mechanisms in the impeller. Since purely theoretical methods have hardly led to any reliable conclusions concerning the criteria of flow separation in the impeller or the secondary character of the impeller flow, there is still little knowledge about the creation of the jet-and-wake zones in the impeller and their decay (associated with large losses) in the connected diffuser. In studying the energy conversion process in the stage as a whole, great attention has to be devoted to the effects of the momentum exchange directly downstream the impeller. Hence the only possible way of solving these problems seems to be specific experimentation. For high flow velocities, this necessitates a special nonsteady measuring technique which also gives information about the relative flow in the rotating impeller.

Contributed by the Gas Turbine Division of The American Society of Mechanical Engineers for presentation at the Gas Turbine Conference & Products Show, Zurich, Switzerland, March 30-April 4, 1974. Manuscript received at ASME Headquarters November 27, 1973.

Copies will be available until December 1, 1974.

THE AMERICAN SOCIETY OF MECHANICAL ENGINEERS, UNITED ENGINEERING CENTER, 345 EAST 47th STREET, NEW YORK, N.Y. 10017

On the Energy Transfer in Centrifugal Compressors

K. BAMMERT M. RAUTENBERG

INTRODUCTION

In developing theoretical methods for realiable design calculations of centrifugal compressors with high stage pressure ratios and high mass flow rates one would have to start (in contrast to the one-dimensional flow theory) from the basic equations for nonsteady, compressible and viscous flow. However, under the conditions stated it is not possible to give a solution of the equation of motion in connection with the continuity equation. Even by neglecting the viscosity influences in the form of friction and by assuming a two-dimensional flow, one does not arrive at a clear-cut solution as the time integrals contained in the set of equations (which are of eminent importance for considering the nonsteady relative flow), are solvable only where the time functions for the various physical quantities are known. However,

NOMENCLATURE

- a = speed of sound
- b = diffuser inlet width
- c = absolute velocity
- D = diameter
- F = fluctuation coefficient ($= 2\,\Delta p_{tot}/\bar{p}_{tot}$)
- f = blade passing frequency ($= z \cdot n/60$)
- M = Mach number ($M_K = c_2/a_K$; $M_u = u_2/a_K$; $M_R = C_2/a_R$)
- $\dot{m}$ = mass flow rate
- n = impeller rotational speed
- p = static pressure
- PS = pressure side (+)
- R = gas constant
- r = radius
- SS = suction side (-)
- s = length of twisted rotor blades at shroud line
- T = absolute temperature or period ($= 1/f$)
- t = time
- u = circumferential velocity
- $\dot{V}$ = volume flow rate
- w = relative velocity
- x/s = related length of twisted rotor blades at shroud line
- y = blade spacing
- z = number of impeller blades or coordinate in axial direction
- α = angle between absolute velocity and the circumferential component
- β = angle between relative velocity and the negative circumferential component
- Δp_{tot} = stochastic fluctuation width of the total pressure $p_{tot}(t)$ at impeller exit
- κ = isentropic exponent
- λ = radius ratio ($= r/r_2$)
- μ = slip factor ($= c_{u2}/c_{u2\infty}$)
- π = pressure ratio
- ρ = density
- φ = inlet flow coefficient $\left(= 4\,\dot{m}/(\rho_1 \cdot \pi \cdot D_2^2 \cdot u_2)\right)$
- ω = angular frequency

Subscripts

- 1 = impeller inlet or blade inlet
- 2 = impeller exit
- ∞ = infinite number of blades
- a = absolute system
- D = diffuser ($\lambda_D = r/r_2 = 1.025$)
- d = design point
- K = equalizing chamber
- Lu = related to Euler work
- M = projected in the meridional plane
- m = meridional
- r = relative system
- s = isentropic
- tot = total
- u = circumferential

Superscripts

- $-$ = time-averaged value
- $\sim$ = fluctuating component

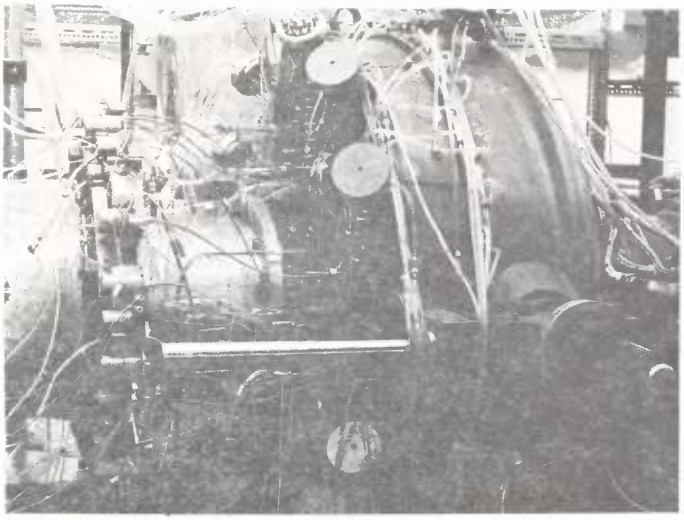

Fig. 1 View of the centrifugal compressor

a possible way to an approximate solution seems to express the mentioned time functions in Fourier Series. The unknown amplitudes and phase angles would have to be determined from measurements and expressed systematically as dimensionless parameters.

Determination of the nonsteady flow mechanism by measurement must be based on knowledge of the local distributions of the various time functions. However, this method raises considerable difficulties since for a blade passage frequency of 6 to 10 kHz direct measurement of velocities and temperatures is hardly possible. For this reason a special analog calculating circuit was conceived and developed (1),[1] which, with the aid of suitable pressure transducers and in connection with hot-wire anemometry, allows all unknown physical quantities to be determined from the measurements. As the transducers used, which are assigned to measure a certain quantity, are sensitive also to other physical quantities, a corresponding calculatory compensation procedure was provided in the analog calculating circuit so that, e.g., a correct evaluation of King's equation, which relates the heat transfer from a hot-wire anemometer to flow and state variables, was possible.

In line with these statements, corresponding measurements of the static pressures, total pressures and the absolute angles of flow were done on a suitable centrifugal compressor, which

[1] Underlined numbers in parentheses designate References at end of paper.

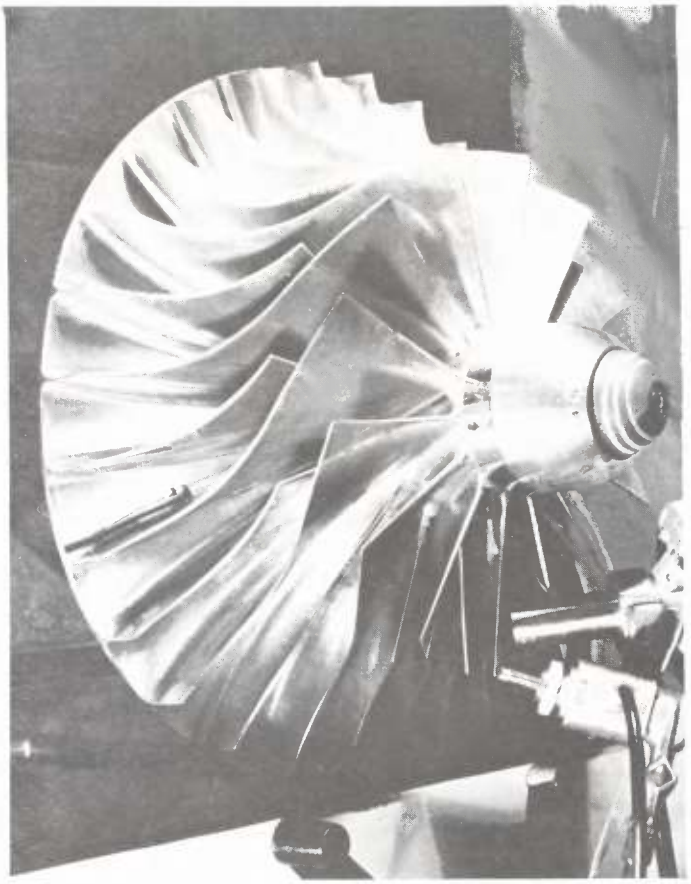

Fig. 2 View of the impeller

allow interpretation of the energy transfer processes in the impeller in accordance with applicable physical laws.

ONE-DIMENSIONAL FLOW THEORY AND NONSTEADY CONSIDERATION

Before dealing with the work carried out and the results obtained, a few words should be said about the necessity of nonsteady approach to the problem. As we know, according to the one-dimensional flow theory it is usual to consider representative mean values of the various physical quantities across the pitch and width and to calculate the work at the impeller circumference with the aid of Euler's equation, viz.

$$\Delta h_{tu} = u_2 \cdot c_{u2} - u_1 \cdot c_{u1} \qquad (1)$$

wherein u_1 and u_2 are the circumferential velocities at the inlet and outlet of the impeller and c_{u1} and c_{u2} the circumferential components of the corresponding absolute velocities.

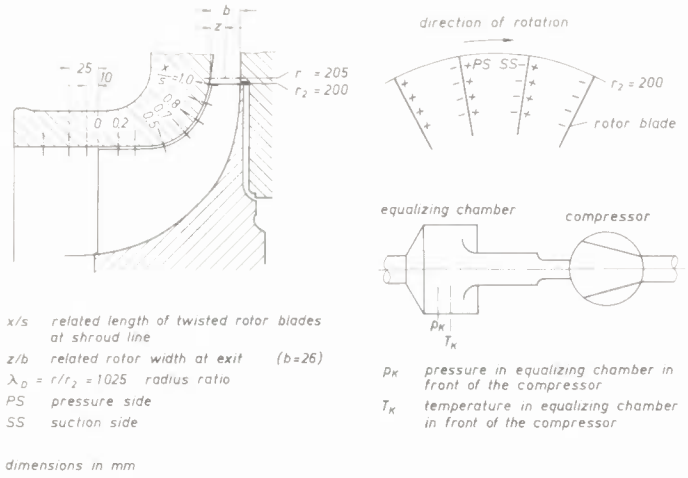

x/s related length of twisted rotor blades at shroud line

z/b related rotor width at exit (b=26)

$\lambda_D = r/r_2 = 1025$ radius ratio

PS pressure side

SS suction side

p_K pressure in equalizing chamber in front of the compressor

T_K temperature in equalizing chamber in front of the compressor

dimensions in mm

Fig. 3 Details and dimensions of the impeller

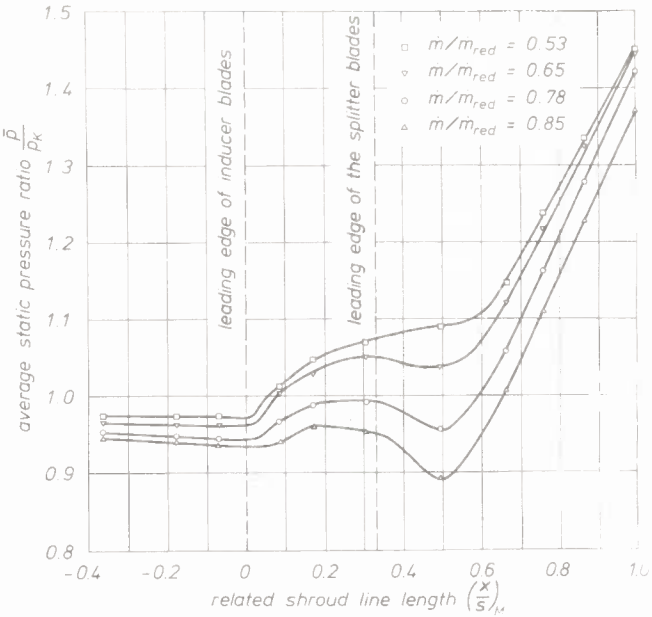

Fig. 4 Static pressure ratio along the shroud line

$n/n_d = 0.78$

Assuming the slip factor to be given by:

$$\mu = \frac{c_{u2}}{c_{u2\infty}} = \frac{c_{u2}/u_2}{1 - \frac{c_{m2}/u_2}{tg\,\beta_{2\infty}}} \qquad (2)$$

and if the losses due to friction and shock are taken into consideration, the total energy transfer in the impeller can be calculated. In equation (2), c_{m2} is the meridional component of the absolute and $\beta_{2\infty}$ the blade angle at impeller exit.

Here already it can be seen how uncertain this method is. In fact, according to the nonsteady energy equation

$$\frac{dh_{tot}}{dt} = \frac{d(h + c^2/2)}{dt} = \frac{1}{\varrho}\frac{\partial p}{\partial t} \qquad (3)$$

a nonuniform pressure distribution in the rotating cascade is required if there is to be any energy transfer at all. In equation (3), h_{tot} is the total and h the static enthalpy, c is the absolute velocity, ρ the density, p the static pressure and t the time.

The pressure gradients as functions of the time, $\partial p/\partial t$, rise with increasing stage loading; as a result there are greater differences in velocity between the blades, which lead to the so-called jet-and-wake effects in the impeller (2) if this velocity differences lead to separation. It is obvious that one can no longer speak of global values of the slip factor or of the circumferential component c_{u2} of the absolute velocity, unless a double integration is made across channel width b and pitch y according to the relation

$$\mu = \frac{2}{\pi}\cdot\frac{z}{\varphi\cdot M_u^2}\cdot\frac{1}{\left(1 - \frac{c_{m2}/u_2}{tg\,\beta_{2\infty}}\right)}\int_{b/D_2=0}^{b_2/D_2}\left\{\int_{y/D_2=0}^{\pi/z}\frac{\varrho}{\varrho_K}\sin 2\alpha\cdot M_K^2\cdot d\,\frac{y}{D_2}\right\} d\,\frac{b}{D_2} \qquad (4)$$

This equation necessitates knowledge of the blade number z, the flow coefficient

$$\varphi = \dot{V}_K \Big/ \left(\frac{\pi}{4} D_2^2 u_2\right)$$

with $\dot{V}_K$ being the suction volume flow rate, the circumferential Mach number $M_u = u_2/a_K$, with

$$a_K = \sqrt{\varkappa \cdot R \cdot T_K}$$

being the velocity of sound upstream the compressor and κ being the isentropic exponent, the

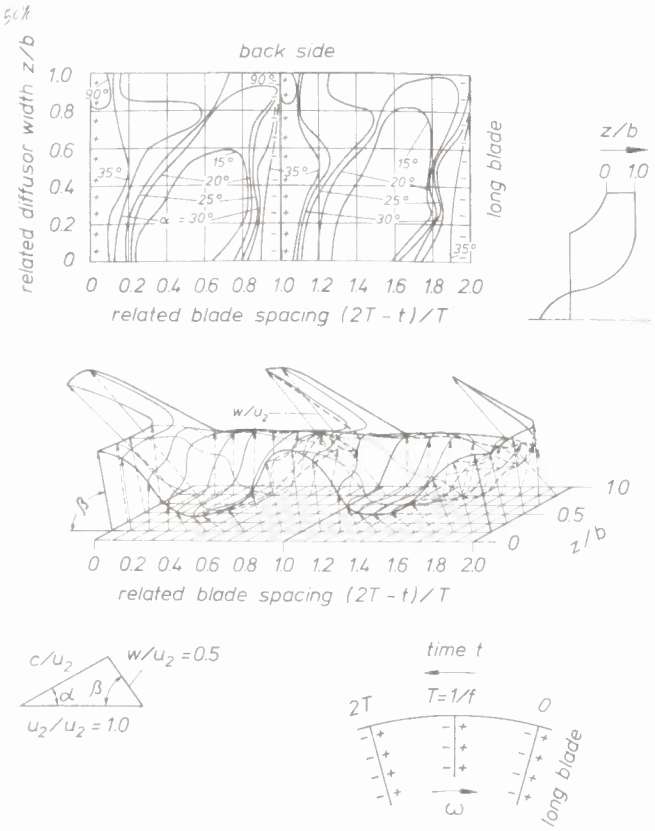

Fig. 5 Relative flow after impeller
$\lambda_D = 1.025$ $n/n_d = 0.78$ $\dot{m}/\dot{m}_d = 0.85$ $z = 28$

densities ρ_K and ρ in the suction chamber and downstream the impeller, respectively, the absolute angle of flow and the Mach number $M_K = c/\sqrt{\kappa \cdot R \cdot T_K}$ based on stagnation temperature T_K. From equation (4) it results that representative calculation of the energy transfer with the aid of the slip factor is only possible if the functional relations to the important characteristic numbers are found by experimentation according to the mechanics of similitude (3). This necessitates an extremely complicated measuring technique and intensive development work on calibrating apparatus.

TEST RIG

In Fig. 1 the front view of the centrifugal compressor with the various measuring taps and probes is shown. For this compressor the 400-mm-dia impeller is shown in Fig. 2, which has so far been operated at circumferential velocities of up to 510 m/sec. The photograph clearly shows the leading edges of the splitter blades of the impeller (total number of blades 28). The inlet diameter is 70 percent of the outlet

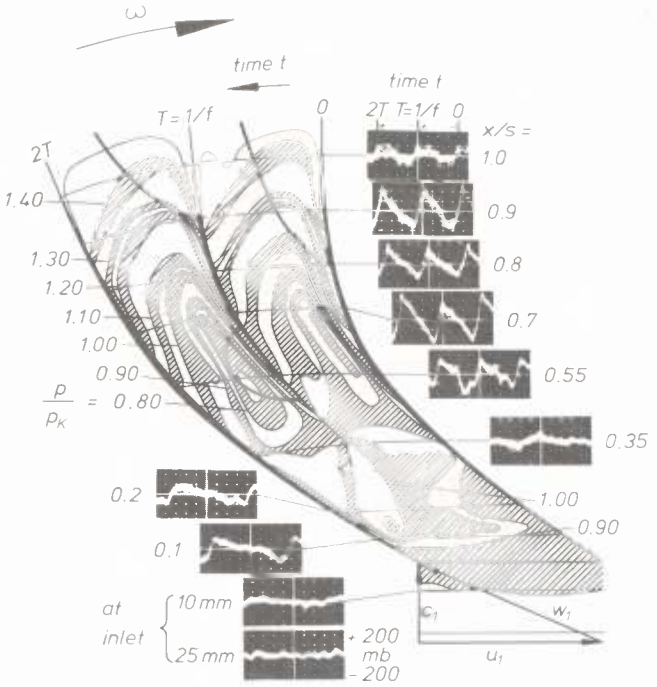

Fig. 6 Static pressure fluctuations and isobars in impeller range
$n/n_d = 0.78$ $\dot{m}/\dot{m}_d = 0.85$ $z = 28$

diameter, and the elliptically twisted blades end absolutely radially.

In Fig. 3 the points of measurements of the steady and nonsteady static pressures in the impeller zone can be seen. The measurements also included the pressures upstream the impeller inlet, where the measuring taps are arranged axially. In the impeller zone the pressure transducers are located along a twisted blade edge length x/s, with x being the coordinate along the twisted blade edge and s the total tip length of an unshortened blade. Downstream the impeller the total pressures p_{tot} and the absolute angles of flow α were measured across the diffuser width b at different intervals z.

STATIC PRESSURE RATIOS ALONG THE IMPELLER SHROUD LINE

Fig. 4 shows the curves of the mean static pressure $\bar{p}$ along the impeller shroud line. This pressure was referred to the pressure p_K in the suction chamber (Fig. 3). These mean pressures were measured pneumatically by means of U pressure gages. The graph shows the related values $\bar{p}/p_K$ plotted against the related blade shroud length $(x/s)_M$ in the meridional plane. For the mass flow rate $\dot{m}/\dot{m}_d = 0.85$ — this case is con-

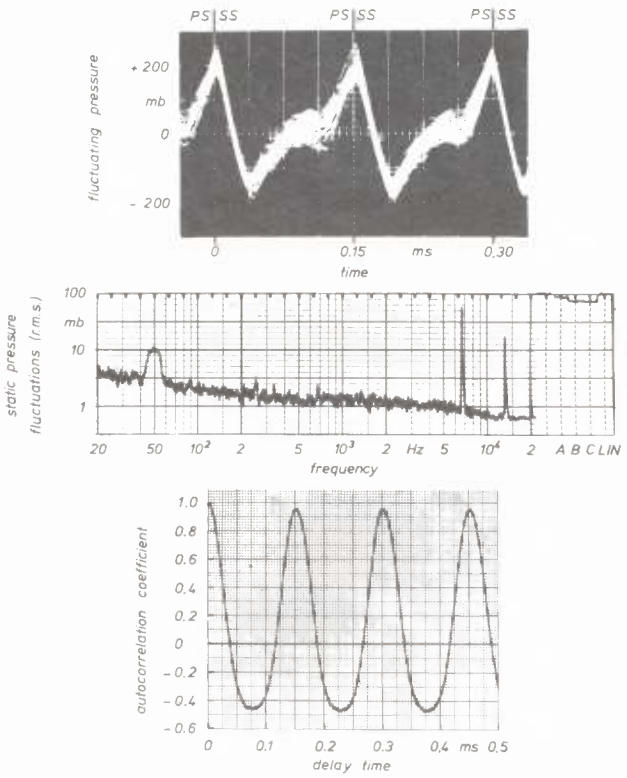

Fig. 7 Analysis of static pressure fluctuations in impeller range
$n/n_d = 1.11$ $\dot{m}/\dot{m}_d = 1.13$ $x/s = 0.8$ $z = 20$

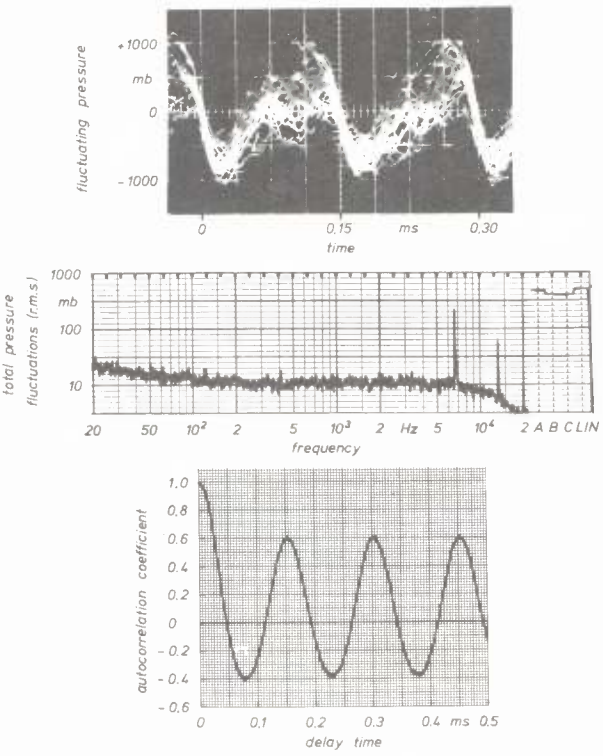

Fig. 8 Analysis of total pressure fluctuations at impeller exit
$n/n_d = 1.11$ $\dot{m}/\dot{m}_d = 1.13$ $\lambda_D = 1.025$ $z/b = 0.10$
$z = 20$

sidered hereafter in connection with the non-steady pressure measurements — there is a pressure peak in the inducer part and a pressure minimum at the starting point of the curvature of the impeller shroud line. This tendency was also detected in the calculation of the axially symmetric flow in the inducer part according to the actuator disk theory (4).

RELATIVE FLOW

As selected example for the development of flow with regard to the distribution of the absolute angle, the isoclinic field in the top part of Fig. 5 is considered. In this graph the lines for constant angles of flow α along the pitch and the width downstream the impeller are shown. These angles of the absolute flow were measured individually with the aid of a hot-wire shadow probe. The borderline between jet and wake zones runs almost diagonally from the pressure side of a blade at the diffuser front wall to the suction side of the neighboring blade at the diffuser back wall. A noteworthy phenomenon is the steep rise of the absolute flow near the back wall on the pressure side of the blade.

From the distributions of the Mach number, which was determined with the aid of an analog calculating circuit from the static and total pressures, and the absolute angle of flow, we determined, e.g., a relative velocity distribution as shown in the middle of Fig. 5. Noteworthy here is the distribution of the relative velocity in the vicinity of the back wall at $z/b = 0.9$ on the pressure sides of the blades. The marked change in direction of the relative-velocity curve is due to the large exit angle at this point. On the pressure side of a blade there is a high mass flow concentration whereas on the suction side of the same blade we have the separation zone. Immediately after leaving the impeller outlet the flow expands into the dead water zone, i.e., the absolute flow shows a very steep rise. This change in direction is the greater the higher the local mass flow is. The picture shows the distributions downstream the impeller; of course, immediately before the impeller exit the relative velocity in the vicinity of the blade pressure side can

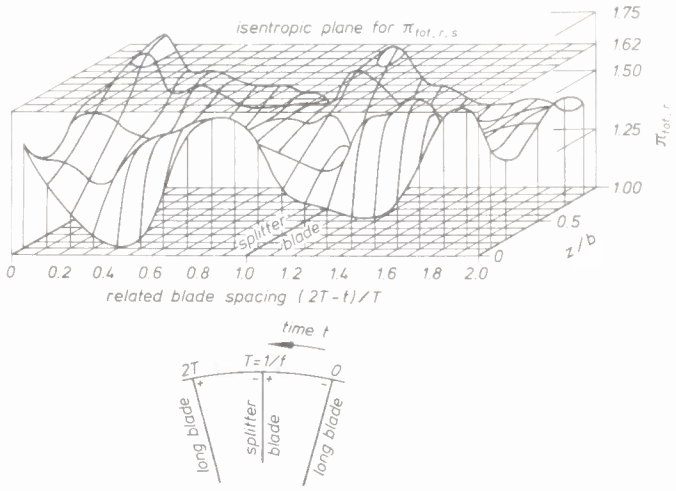

Fig. 9 Distribution of the total pressure in a relative system
$n/n_d = 0.78$ $\dot{m}/\dot{m}_d = 0.85$ $\lambda_D = 1.025$ $z = 28$

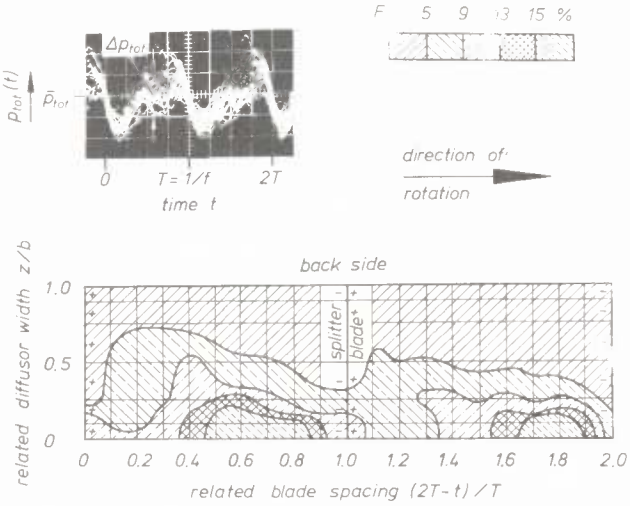

Fig. 10 Fluctuation coefficient F for total pressure $p_{tot}(t)$
$n/n_d = 0.78$ $\dot{m}/\dot{m}_d = 0.85$ $\lambda_D = 1.025$ $z = 28$

be parallel to the blade at the most.

SEPARATIONS OF FLOW IN THE IMPELLER

From the curves of the nonsteady static pressures along the impeller shroud line, whose oscillograms were related to the various points of measurement in the channels, one can first prepare the isobaric field as shown in Fig. 6. One can clearly see the pressure stagnation upstream the splitter blade and a shift of the stagnation zone to the pressure side of the long blade. On the blade suction sides marked pressure decreases were measured, which are accompanied by considerable accelerations of the flow. The results shown in Fig. 6 were obtained for a related mass flow rate of $\dot{m}/\dot{m}_d = 0.85$ and a related dimensionless r.p.m. of $n/n_d = 0.78$ with $\dot{m}_d$ and n_d being the data for the nominal design point. The result of the mass flow integration for this operating point was that the mass flow in the left-hand channel was slightly above that in the right-hand channel. With lower mass flow rates the conditions were reversed.

In the isobaric field, the limits of the dead water zones determined from the curves of nonsteady pressure and the locations of the separation points were drawn. It was assumed that in the wake zone there is an almost constant static pressure in circumferential direction. From the oscillograms such zones can be clearly detected. On the suction side of the splitter blade one can see a separation bubble. When comparing the widths of the zones of separation found here with the widths of the jets and wakes in the representation of the relative flow (Fig. 5) one can see that the conditions in the vicinity of the front casing wall are very much the same.

ANALYSIS OF THE PRESSURE SIGNALS

The stability of static pressure signals, which were used for preparing the isobaric fields and are decisive for the energy transfer in the cascade, can be shown, e.g., with the aid of the oscillogram at the top of Fig. 7 for $n/n_d = 1.11$. In the oscillogram about 50 superimposed passage signals for two specific blade channels of an impeller with 20 blades of equal length are shown. At the top edge of Fig. 7 the locations of the blades and the abbreviations PS for the pressure side and SS for the suction side of the blades are shown. One can distinguish a highly periodic signal with a narrow stochastic deviation range, which is confirmed in the narrow-band spectrum by comparatively low effective values for the low-frequency broad-band spectrum. The rise of rms-value of static pressure peak at the frequency of 50 Hz was caused by interference voltage in the measuring system. The oscillating pressure is almost exclusively determined by the discrete frequencies of the blade passage frequency and its higher harmonics. The period of 0.15 msec is identical with the blade-to-blade time interval. In the bottom part of

Fig. 7 the autocorrelation coefficient of 95 percent indicates a very high degree of interrelation. It thus shows extraordinary stability of the signal reproduction.

An output calculation via the slip factor necessitates, apart from measurement of the absolute angles of flow, in particular determination of the total pressure oscillations at the impeller outlet, for which in Fig. 8 an example is shown again with $n/n_d = 1.11$ This signal was picked up in the vicinity of the front wall on a 20-blade impeller at $z/b = 0.10$ and thus reflects mainly the flow conditions near the clearance between impeller and casing. Unlike the static pressure oscillogram, the total-pressure oscillogram in the top part of the picture shows a much wider stochastic deviation. In the narrow-band spectrum there is a wider frequency band with an almost constant effective value of 20 Hz up to the frequency of the blade passage frequency, and the autocorrelation coefficient is only up to 0.60, which also indicates a less precise fixation of time axis and a much reduced stability of the flow. Only real-time analyses of these pressure signals will permit conclusions about the character and degree of the nonsteady relative flow. The reason for this is that, e.g., the stochastic deviation ranges in the oscillogram as shown in Fig. 8 cover not only absolute, global fluctuations of flow (fluctuations of the operating point) but in particular also periodic instabilities in the relative system, periodic separations of boundary layers at the blade walls and general turbulences in the relative system.

RELATIVE TOTAL PRESSURE RATIO

A measure of the energy distribution at the impeller outlet is the relative total pressure ratio $\pi_{tot,r}$. For the impeller shown in Fig. 2, the relative total pressure ratio across two blade pitches and across the impeller outlet width is shown in a three-dimensional form (Fig. 9). For this particular impeller ($\beta_{2\infty} = 90$ deg) with swirl-free flow ($c_{u1} = 0$), the relative total pressure $\pi_{tot,r}$ may be written as:

$$\pi_{tot,r} = \pi_{tot,a} \cdot \left[1 - \frac{\varkappa - 1}{2} \left(\frac{M_u \cdot M_R}{M_K} \right)^2 \right]^{\frac{\varkappa}{\varkappa - 1}} \qquad (5)$$

In this derivation, we have used the transformed total enthalpy (5) defined as:

$$\bar{h} = h + \frac{w^2}{2} - \frac{u^2}{2} \qquad (6)$$

which is assumed to be constant in the impeller, in connection with the relative total enthalpy defined as:

$$h_{tot,r} = h + \frac{w^2}{2} \qquad (7)$$

In equation (5) $\pi_{tot,a} = p_{tot}/p_K$ is the absolute total pressure ratio as determined from the measured total pressures p_{tot} downstream the impeller (Kiel probe) and p_K in the suction chamber upstream the compressor, and M_R Mach number referred to the local velocity of sound $a_R = \sqrt{\kappa \cdot R \cdot T_{tot}}$, with T_{tot} being the absolute total temperature. For the isentropic flow with the slip factor $\mu = 1$ ($z =$) there then results the isentropic relative total pressure ratio

$$\pi_{tot,r,s} = \left[1 + \frac{\varkappa - 1}{2} \cdot M_u^2 \right]^{\frac{\varkappa}{\varkappa - 1}} \qquad (8)$$

whose value of 1.62 was determined for this particular circumferential Mach number M_u. The isentropic plane formed in this manner (Fig. 9) is pierced in the zone of the blade pressure side and more in the vicinity of the channel back wall by the $\pi_{tot,r}$ peaks.

Originally a measuring error was assumed as there was no theoretical explanation for such an intensive energy exchange in the fluid within the rotating cascade. Similar measurements at other points (6 and 7) and frequent repeat measurements soon proved that the possibility of measuring errors was to be excluded. On the basis of turbulences in the relative system and taking into account the Coriolis forces one may assume a division of energy between the core flow on the pressure side and the wake flow on the suction side of a blade channel.

In this connection there at once arises the question as to the turbulence and the nonsteady character of the flow in the relative system. Assuming that the stochastic deviation range of the total pressure at the impeller outlet is a certain measure of nonsteady relative flow, a fluctuation factor

$$F = \frac{\Delta p_{tot}/2}{\bar{p}_{tot}} \qquad (9)$$

can be defined, with Δp_{tot} being the maximum stochastic deviation range and $\bar{p}_{tot}$ the mean value of the total pressure $p_{tot}(t)$ at the impeller outlet. This fluctuation factor as shown in Fig. 10 represents to some extent a degree of turbulence of the relative flow. In the zone of the front wall, i.e., in the zone of the blade-to-blade clearances, it is up to 20 percent. The measurements of Fowler (8) show similar effects.

It is doubtful whether this fluctuation can be interpreted as indicating turbulence in the relative system. There is rather reason to assume that the fluctuation factor thus determined is to be considered as a conglomerate of all the instabilities, turbulences and other, perhaps periodic, separations and disturbances. A reliable interpretation of these phenomena will only be possible through systematic analysis of the signals in the form of real-time Fourier analyses. This is the path that should be followed.

SUMMARY

The statements made in the preceding part give only a brief survey of the work done in the past and thus also convey an impression of the extremely complex flow conditions in the impeller of a highly loaded centrifugal compressor stage. Great efforts will still be necessary if one wants to arrive at optimum flow conditions at still higher handling capacities. Among the main difficulties to be solved are the problems of measuring technique, the development of suitable testing and calibration equipments and the necessity of a more precise real-time analysis in high frequency ranges. But also the material strength problems and further questions relating to the dynamic behavior of such a machine set are of great importance. Similar difficulties are presented by the physical effects of momentum exchange directly at the impeller outlet, which have a great influence on the further conversion of energy in the diffuser. In this connection the nonsteady processes on development and disappearance of the boundary layers play an important part. Therefore, a theory for dealing with the complex flow conditions in the impeller must be based on experimentally found knowledge and its physical side must also cover the unsteady flow conditions in the relative system, including the separation criteria, to ensure that also the extremely difficult but highly important effects of energy distribution in the cascade are considered.

ACKNOWLEDGMENTS

The existing experimental results were obtained from a centrifugal compressor test rig which was conceived by German turbo compressor manufacturers and whose construction was financed by the Forschungsvereinigung Verbrennungskraftmaschinen e.V. (FVV). The extremely complicated electronic measuring technique required for it was developed and financed within the framework of the research work covered by the Sonderforschungsbereich 61 (special research field). The authors gratefully acknowledge the valuable assistance granted by the Verein Deutscher Maschinenbau-Anstalten (VDMA) as the parent organization of the FVV and AIF (Arbeitsausschuß für industrielle Forschung) and by the Deutsche Forschungsgemeinschaft.

REFERENCES

1 Bammert, K., and Rautenberg, M., "Messung zeitlich veränderlicher Strömungsvorgänge im Radialverdichter," VDI-Berichte, No. 193, 1973, pp. 187-196.

2 Dean, R. C., and Senoo, Y., "Rotating Wakes in Vaneless Diffusors," Trans. ASME, Basic Engineering, Vol. 82, No. 3, 1960, pp. 563-574.

3 Bammert, K., and Rautenberg, M., "Zur Ähnlichkeitsmechanik von Turboverdichtern," Wärme, Vol. 74, No. 1/2, 1968, pp. 37-51.

4 Schröder, H. J., "Die Wirbelscheibenmethode in Anwendung auf die Drallströmung durch axiale Turbomaschinen," Fortschritt-Berichte der VDI-Z, Reihe 7, No. 28, 1972.

5 Bammert, K., and Fiedler, K., "Die Strömung in axialen Turbomaschinen," Ingenieur Archiv, Vol. 33, 1964, pp. 322-329.

6 Prian, V. D., and Michel, D. J., "An Analysis of Flow in Rotating Passage of Large Radial-Inlet Centrifugal Compressor at Tip Speed of 700 Feet per Second," NACA-TN 2584, 1951.

7 Fette, H., "Strömungsversuche im rotierenden Laboratorium," Z. Techn. Physik, 14, Jahrg, 1933.

8 Fowler, H. S., "An Investigation of the Flow Processes in Centrifugal Compressor Impeller," National Research Council of Canada, Rep. ME-229, Ottawa, 1969.